Am J Cancer Res 2023;13(4):1560-1570
www.ajcr.us /ISSN:2156-6976/ajcr0147944

Original Article

CgB promotes EMT and stemness via MAPK pathway in colonic neuroendocrine carcinoma

Junpeng Cui[1], Yang Ge[1], Wei Sun[1], Baolin Liu[1], Chaoliu Dai[2]

[1]Department of Sixth General Surgery, Shengjing Hospital Affiliated to China Medical University, Shenyang 110004, Liaoning, China; [2]Department of Fifth General Surgery, Shengjing Hospital Affiliated to China Medical University, Shenyang 110004, Liaoning, China

Received November 22, 2022; Accepted April 3, 2023; Epub April 15, 2023; Published April 30, 2023

Abstract: The incidence of colorectal neuroendocrine tumors is increasing every year with poor prognosis. Members of Chromogranin family proteins have been shown to be associated with cancer metastasis; however, the role of chromogranin B in colonic neuroendocrine carcinoma (NEC) is unknown. In this study, we investigated the expression and function of CgB in colonic NEC. Using RNA-seq data from GSE 9576 and GSE 142720 datasets, we analyzed the differentially expressed genes between the normal and NEC samples, which protein levels were further validated using the Human Protein Atlas (HPA) databases. Moreover, immunohistochemistry staining and biological experiments were conducted to examine the expression and function of CgB in colonic NEC. Western blot was also performed to confirm the effect of CgB on epithelial mesenchymal transition (EMT) and its related pathways. We found that the expression level of CgB was significantly higher in colonic NEC tissues than in the adjacent tissues. The upregulation of CgB promoted cell invasion and migration as well as activated EMT and stemness. Mechanistically, both pathway enrichment analysis and Western blot analysis confirmed that CgB overexpression activated p38 MAPK and ERK pathways, while silencing CgB showed the opposite effects. Collectively, our results suggested that CgB activated p38 MAPK and ERK pathways, thereby contributing to the development of colonic NEC.

Keywords: Chromogranin B, colonic neuroendocrine carcinoma, mitogen-activated protein kinase

Introduction

Colorectal neuroendocrine neoplasms (NENs) are tumors of epithelial cell origin with morphological and immunophenotypic signs of neuroendocrine differentiation and can be classified into neuroendocrine tumor (NET), neuroendocrine carcinoma (NEC), and mixed neuroendocrine-non neuroendocrine neoplasm (MiNEN). Among them, colonic MiNEN is the most common type followed by colonic NEC [1]. Colorectal NENs are highly malignant and invasive with high liver metastasis and poor prognosis [2, 3].

Chromogranin B (CgB), a soluble, acidic, and specific neuroendocrine protein, belongs to the acidic secretory protein family with chromaffin A (CgA) and secretogranin II that are widely present in mammalian neuroendocrine cells [4]. CgA and CgB are similar in structure, with a homologous disulfide ring structure at the N-terminal and another homologous sequence at the C-terminal, suggesting that they may have evolved from a common origin. Human CgB gene is located on chromosome 20 and is composed of 677 amino acids in five exons [5, 6]. The structure features of CgB include a large number of acidic amino acids, calcium binding sites, and several potential binary cleavage sites. In addition, CgB is post-translationally modified at many sites and has a tendency of self-aggregation [7]. Functionally, Chromogranin family has been shown to promote the regulatory secretion of polypeptides, hormones, neurotransmitters, and growth factors [8, 9]. Nevertheless, the role of CgB in patients with colonic NEC has not been reported. In this study, we explored the expression of CgB in colonic NEC by using the clinical samples and analyzed its correlation with the pathological features. Furthermore, we determined the function and the underlying mechanism of CgB in the progression of NEC.

Materials and methods

Patient samples

In this study, 30 specimens were randomly collected from colonic NEC patients of 13 males and 17 females aged of 46-82, who were treated in the sixth general surgery of Shengjing Hospital Affiliated to China Medical University. All tumor stages were determined according to the latest version of American Joint Cancer Committee/Union for International Cancer Control TNM staging standard for colorectal tumor. All patients signed informed consent forms, and the study was approved by the Ethics Committee of Shengjing Hospital Affiliated to China Medical University (2022PS1128K).

Bioinformatics analysis

Data from GSE9576 and GSE142720 datasets in Gene Expression Omnibus (GEO) database (https://www.ncbi.nlm.nih.gov/geo/) were downloaded and analyzed in this study. R package was utilized to identify differentially expressed genes and to draw a heat map. In addition, we retrieved immunohistochemical (IHC) images of colonic NEC from the Human Protein Atlas (HPA) database (http://www.proteinatlas.org). In the HPA database, genome-wide transcriptomics data and clinical metadata of nearly 8000 patients were used to analyze the proteome of major diseases [10]. According to the median expression of CgB, the data were divided into high- and low-CgB expression groups. To investigate the differentially activated pathways between the high- and the low-CgB expression groups, the Gene Set Enrichment Analysis (GSEA) was performed for enrichment analysis, and the enrichment of known pathway gene sets in the two groups was compared.

Cell lines and cultures

Human colonic NEC cell line LCC-18 was purchased from Shanghai Enzyme Biotechnology. LCC-18 cells were cultured in RPMI 1640 medium containing 10% fetal bovine serum and maintained at 37°C with 5% CO_2. The cells were transfected with lentivirus expressing CgB (LV-CgB OE group for CgB overexpression) or shCgB (LV-shCgB group for CgB silencing). The shCgB sequence is gGCTGCTGCTGTTGCTGCTGCTttcaagagaAGCAGCAGCAACAGCAGCAGCttttt. The overexpression or silencing of CgB was confirmed by PCR using the following conditions: pre-denaturing at 95°C for 2 min, denaturing at 95°C for 15 s, annealing at 58°C for 30 s, extending at 72°C for 30 s, and cycling for 42 times.

Immunohistochemistry staining

IHC was performed with CgB antibody (Affinity, China), and the IHC staining signal were scored by two experienced pathologists independently. The immunohistochemical score was calculated by the staining intensity and the percentage of stained cells. The staining intensity was graded as strong (3 points), moderate (2 points), weak (1 point), and negative (0 point). The percentage of positive cells was scored as 4 points (more than 75%), 3 points (50-75%), 2 points (26-50%), 1 point (1-25%), and 0 point (negative). The total score of up to 3 points was considered positive.

Real-time quantitative PCR (RT-qPCR)

The transcript level was determined by RT-qPCR using SYBR Premix Ex TaqII on ABI QuantStudio 5 Real time PCR, and $2^{-\Delta\Delta Ct}$ was calculated for the relative quantitation analysis. Primer sequences used in this study were listed in Supplementary Table 1.

Transwell assay

The invasion of transfected cells was determined by transwell assay. Briefly, cells in serum-free medium were seeded into the upper chamber of Transwell, while complete medium was added to the lower well. After 24 h of culture, the top side of the upper chambers was gently swabbed with cotton-tipped applicators, and then the chamber was fixed with paraformaldehyde for 30 min followed by 0.1% crystal violet staining for 20 min. Transwells were observed under 400 × microscope, and the cells in five randomly selected fields were counted.

Wound healing assay

The migration of LCC-18 cells was access by wound healing assay. Briefly, cells at 90% confluence were scratched with a 200 μl pipette tip and washed with PBS. The cells were photographed as 0 h and cultured for 24 h. Images were then acquired at 24 h. The wound closure was calculated by the difference in the width between time 0 and at 24 h of culture.

Western blot

Protein sample preparation: briefly, RIPA buffer (containing proteinase inhibitor PMSF) was used to lyse cells and the cell lysate was cleared by centrifugation at 4°C for 30 min. The supernatant was collected, quantified, and separated by SDS-PAGE. Proteins were then transferred onto PVDF membrane followed by standard western blot procedure. Primary antibodies used in this study were: p38 antibody (Cell signaling), p-p38 antibody (Cell signaling), ERK antibody (Cell signaling), p-ERK antibody (Cell signaling), CgB antibody (Abclonal), GAPDH antibody (Cell signaling), E-Cadherin antibody (Wuhan Sanying), Vimentin antibody (Wuhan Sanying) and SOX2 antibody (Wuhan Sanying). Corresponding HRP-linked anti-IgG antibody (Cell signaling) was used as the second antibody. ECL solution was used to develop the specific protein signal, and the protein expression was semi-quantitatively analyzed by Image J software.

Subcutaneous xenograft tumor model in nude mice

Male BALB/c nude mice (4-6 weeks old) were purchased from Beijing Vital River Laboratory Animal Technology Co., Ltd. and were used in this study. To generate xenograft tumors, LCC-18 cells (10^6/100 ul PBS) were inoculated subcutaneously into the flank of nude mice (n=4/group). The tumor growth was monitored every 7 days, and the tumor volume was calculated according to the following formula: 0.5 × (length × width)^2. At week 4 after cell injection, the mice were sacrificed, and the tumor was dissected for further analysis. All animal handling was in accordance with the policies and procedures of the National Institutes of Health's Guidelines for the Care and Use of Laboratory Animals. The animal protocol was approved by the Ethics Committee of Shengjing Hospital Affiliated to China Medical University (2022-PS1165K).

Statistical analysis

SPSS 20.0 and GraphPad Prism 8.0 were utilized for statistical analysis and mapping. Continuous variables were expressed as mean ± standard deviation. Counting data were expressed as rate. Independent sample *t*-test was used to compare the differences between the two groups, while one-way analysis of variance and Bonferroni-corrected *t*-test were used to compare the difference among multiple groups. Chi-square test was used to compare the expression level of CgB and its relationship with clinical data. P<0.05 was considered statistically significant.

Results

The differential expression of CgB between carcinoma and the adjacent tissues

Two datasets (GSE142720 and GSE9576) related to intestinal neuroendocrine tumors in GEO database were selected to explore the expression of CgB, and cluster thermogram was utilized to display the differential expression between NEC and the normal tissue, with red representing high while green representing low expression (**Figure 1A**). The results showed that the expression of CgB was significantly higher in colonic NEC than in the adjacent normal tissues (P=0.012). Consistently, the IHC staining results in HPA database also proved the upregulation of CgB expression (**Figure 1B**).

Furthermore, using the median CgB expression as the cutoff value, the transcriptome expression profile in the database was divided into high- and low-expression groups, and the GSEA analysis was performed. We found that mitogen-activated protein kinase (MAPK) pathway was significantly activated in the CgB high-expression group (NES=0.901, FDR q value =0.65) (**Figure 1C**).

More importantly, we examined the expression of CgB in our own 30 clinical NEC samples by IHC (**Figure 1D**) and found that 17 cases (56.7%) were positive for CgB staining, whereas only 7 cases (23.3%) in the adjacent tissues were positive for CgB staining, further supporting the conclusion of the upregulation of CgB in NEC (P=0.008).

Relationship between CgB expression and clinical parameters

Next, we found that the expression of CgB was related to TNM stage, lymphatic metastasis, and distant metastasis. Specifically, as shown in **Table 1**, the positive CgB expression rate was 30% and 70% in stage I/II group and stage III/IV group, respectively (P=0.037). In addition,

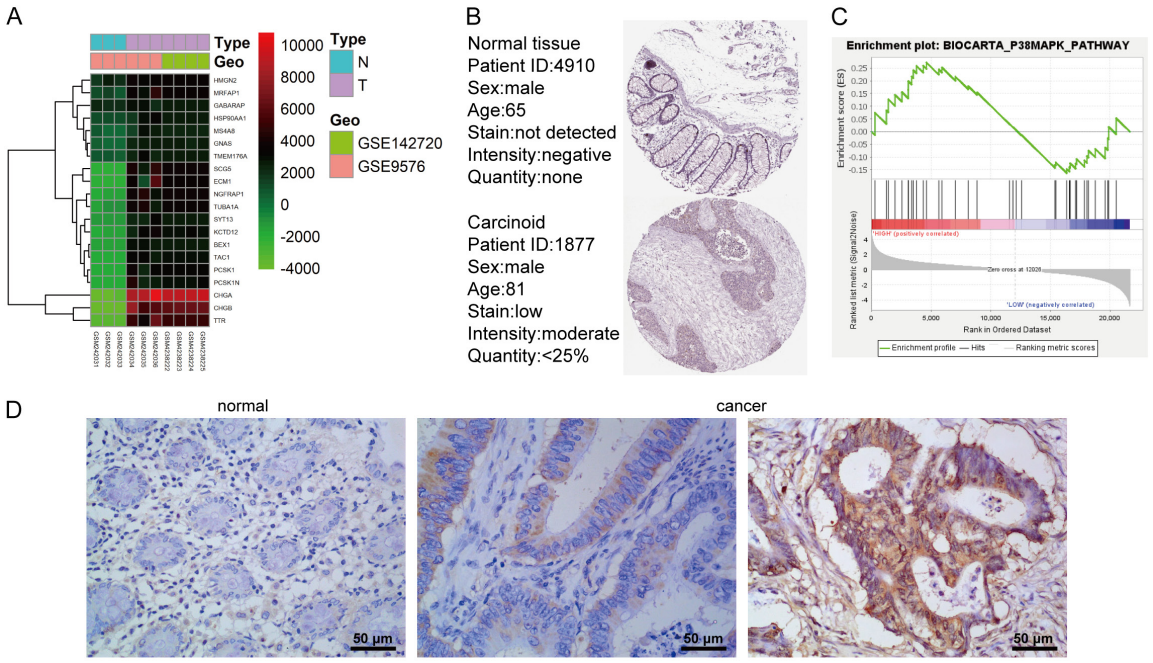

Figure 1. Differential gene expression as well as the enrichment of signal pathways between carcinoma tissues and the adjacent tissues. A. Cluster thermogram of differential gene expression in tissues in GEO database. B. IHC staining results of HPA database. C. GSEA enrichment analysis showed that MAPK pathway was significantly activated in high-CgB expression samples. D. IHC staining results of CgB in patient tumor samples and adjacent tissues.

the positive CgB expression rate was 71.43% in the lymph node metastasis group but was only 22.22% in the non-lymph node metastasis group (P=0.013). Similarly, the positive CgB expression rate was 75% in the group with distant metastasis while was only 35.71% in the group without distant metastasis (P=0.03). Notably, the positive CgB expression rate was as high as 84.62% in the death group but was only 35.29% in the survival group (P=0.01).

Establishment of cell lines with CgB overexpression or silencing

To investigate the function of CgB in NEC, we established LCC-18 cells with CgB overexpression (LV-CgB OE) or silencing by shRNA (LV-shCgB) via the transfection of corresponding lentivirus plasmids. PCR was performed to verify the overexpression or silencing of CgB. The relative expression of CgB mRNA in LV-CgB OE transfection group and NC group was 3.558±0.598 and 1.001±0.063, respectively (P=0.002), while the relative expression of CgB mRNA in LV-shCgB group and LV-shRNA-NC group was 0.541±0.113 and 1.237±0.179, respectively (P=0.005).

CgB promoted xenograft tumor growth in vivo

As shown in **Figure 2**, compared with the control group, the volume of the subcutaneous tumors derived from CgB overexpressing cells was significantly larger than that in the control group, while the volume of tumors derived from CgB silencing cells was significantly smaller than that in the control group (276.39±31.01 vs 162.67±41.85, P=0.005; 46.06±12.80 vs 149.85±51.52, P=0.008). Consistently, the weight of CgB-overexpressing tumors was significantly higher than that in control group, while the weight of CgB-silencing tumors was significantly lower than that in control group (0.38±0.05 vs 0.21±0.04, P=0.001; 0.11±0.08 vs 0.21±0.03, P=0.001).

CgB promoted cell invasion and migration in vitro

Transwell invasion assay and wound healing assay were performed to assess the effect of CgB on the invasion and migration of NEC cells, respectively. The results showed that CgB overexpression enhanced, while CgB silencing inhibited cell invasion and migration. As shown in **Figure 3**, a statistically significant difference

Table 1. Relationship between CgB expression and the clinical features in patients with colonic NEC

Clinical features	n	%	CgB		P
			Positive (n=17)	Negative (n=13)	
age					
≤65	15	50	10 (66.67%)	5 (33.33%)	0.269
>65	15	50	7 (46.67%)	8 (53.33%)	
gender					
male	13	43.33	8 (61.54%)	5 (38.46%)	0.638
female	17	56.67	9 (52.94%)	8 (47.06%)	
pathological grading					
grade I	0	0	0	0	0.713
grade II	24	80	14 (58.33%)	10 (41.67%)	
grade III	6	20	3 (50%)	3 (50%)	
TNM					
I-II	10	33.33	3 (30%)	7 (70%)	0.037*
III-IV	20	66.67	14 (70%)	6 (30%)	
invasion depth					
T1-T2	2	6.67	1 (50%)	1 (50%)	0.981
T3	21	70	12 (57.14%)	9 (42.86%)	
T4	7	23.33	4 (57.14%)	3 (42.86%)	
lymphatic metastasis					
yes	21	70	15 (71.43%)	6 (28.57%)	0.013*
no	9	30	2 (22.22%)	7 (77.78%)	
distant metastasis					
yes	16	53.33	12 (75%)	4 (25%)	0.03*
no	14	46.67	5 (35.71%)	9 (64.29%)	
dead or not					
yes	13	43.33	11 (84.62%)	2 (15.38%)	0.01*
no	17	56.67	6 (35.29%)	11 (64.71%)	

*: P<0.05.

between CgB overexpression group and control group was observed for both invasion (1049±106 vs 456±46, P=0.001) and migration (67.78±2.18 vs 45.74±2.05, P<0.001). Similarly, the difference between the CgB silencing cells and the control cells in invasion (160±25 vs 380±36, P=0.001) and migration (18.42±1.15 vs 42.67±0.55, P<0.001) was also statistically significant.

CgB promoted epithelial-mesenchymal transition (EMT) and stemness via p38 MAPK and ERK pathways

Given the data above showing the enhanced invasion and migration ability by CgB, we speculated that overexpression of CgB might promote EMT. Hence, the expression of EMT-related proteins E-cadherin and Vimentin as well as the stemness-related protein SOX2 were determined by Western blot. As shown in **Figure 4A**, the expression of E-cadherin was decreased significantly while the expression of Vimentin and SOX2 was increased significantly by the overexpression of CgB. Conversely, CgB silencing resulted in the opposite effects. We further explore the mechanisms underlying the function of CgB. As shown in **Figure 4B**, overexpression of CgB significantly increased, while CgB silencing suppressed, the expression of p-p38 and p-ERK; however, the total p38 and ERK protein levels were not affected. In support with these findings, the results from xenograft tumor samples also verified that CgB promoted the activation of MAPK pathway (**Figure 4C**).

Effect of inhibiting p38 MAPK and ERK pathways on LCC-18 cells

To further investigate the functional importance of ERK and p38 activation in mediating

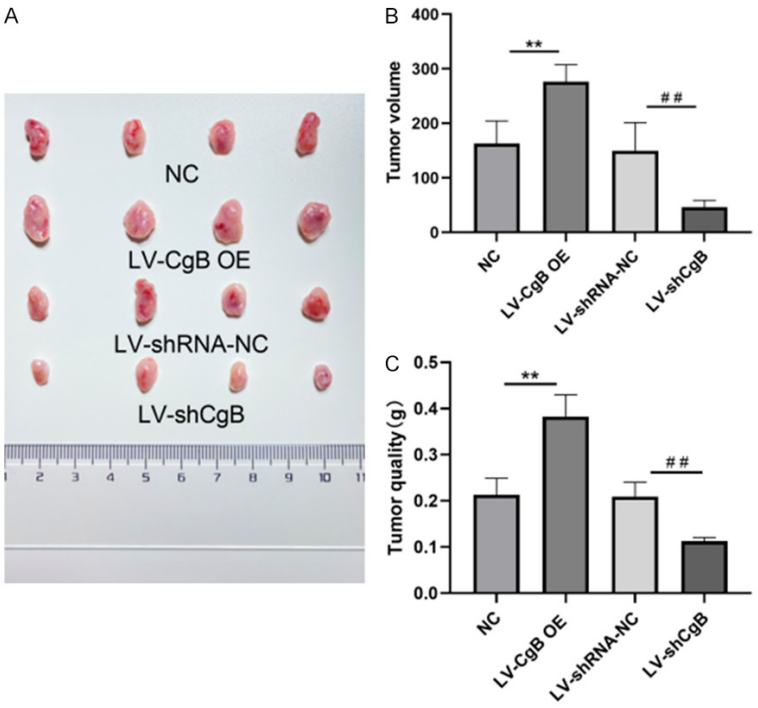

Figure 2. CgB promoted xenograft tumor growth in vivo. A. Tumor growth after subcutaneous injection in nude mice. Tumor volume was increased in CgB-overexpressed group but decreased in CgB-silencing group. B. The bar graph of tumor volume in each group, showing the statistically significant difference. C. Bar graph of tumor weight in each group, and the difference was statistically significant. **: P<0.01; ##: P<0.01.

CgB activity, we treated LCC-18 cells with ERK pathway inhibitor U0126 (10 μM) and p38 pathway inhibitor SB202190 (20 μM) for different times: 6 h, 12 h, 24 h and 48 h, and then detected the proliferation of LCC-18 cells by CCK-8 assay. As shown in **Figure 5A**, cell proliferation was inhibited by 24 h treatment of U0126 and SB202190, as the OD value was significantly lower in inhibitor-treated cells than in the control cells (P=0.04 and P=0.017). Longer treatment of 48 h further increased the difference in the OD value between the two groups (both P<0.001). Furthermore, ERK pathway was significantly inhibited by 12 h of U0126 treatment. Meanwhile, E-cadherin expression was increased, while Vimentin expression was decreased, suggesting the involvement of ERK signaling pathway in CgB-regulated EMT process (**Figure 5B**). Similarly, 12 h of SB202190 intervention significantly inhibited p38 pathway. The expression of E-cadherin was also increased, while the expression of Vimentin was decreased, suggesting that the p38 signaling pathway was also involved in CgB-regulated EMT process (**Figure 5C**).

Discussion

In this study, we revealed that CgB may play an important role in the occurrence and progression of colonic NEC. We found an upregulation of CgB in colonic NEC, possibly by the activation of MAPK pathway, and the high level of CgB expression promoted the progression of NEC. Hence, our study suggested that CgB might serve as a novel biomarker for the diagnosis and treatment of colonic NEC.

It has been reported that in patients with pancreatic cancer, serum CgB levels can be used to differentiate pancreatic neuroendocrine tumors from other pancreatic diseases, and the plasma CgB concentrations returns to normal after successful tumor resection [11, 12]. In gastrointestinal neuroendocrine tumors, the diagnostic sensitivity of circulating CgB detection is similar to that of CgA, but it can avoid the influence from the decline of renal function and the effect of proton pump inhibitor treatment; therefore, it can be used as an important tumor marker of neuroendocrine tumors [13]. In addition, a recent study found that CgB level was significantly correlated with the pathological grade and liver metastasis of pancreatic and rectal neuroendocrine tumors. Since the pathological grade and tumor load of liver metastasis are negatively correlated with the prognosis of patients, serum CgB may become a potential prognostic marker [14]. In consistent with these findings, our data also showed that the positive expression rate of CgB was higher in colonic NEC tissues than in the adjacent tissues.

EMT refers to the process by which epithelial cells transform into mesenchymal cells through specific pathways under normal or pathological conditions, showing stronger migration and invasion ability. The decreased expression of E-cadherin is the most important marker of EMT [15]. On the other hand, tumor stem cells are a specific subset of cells that have the

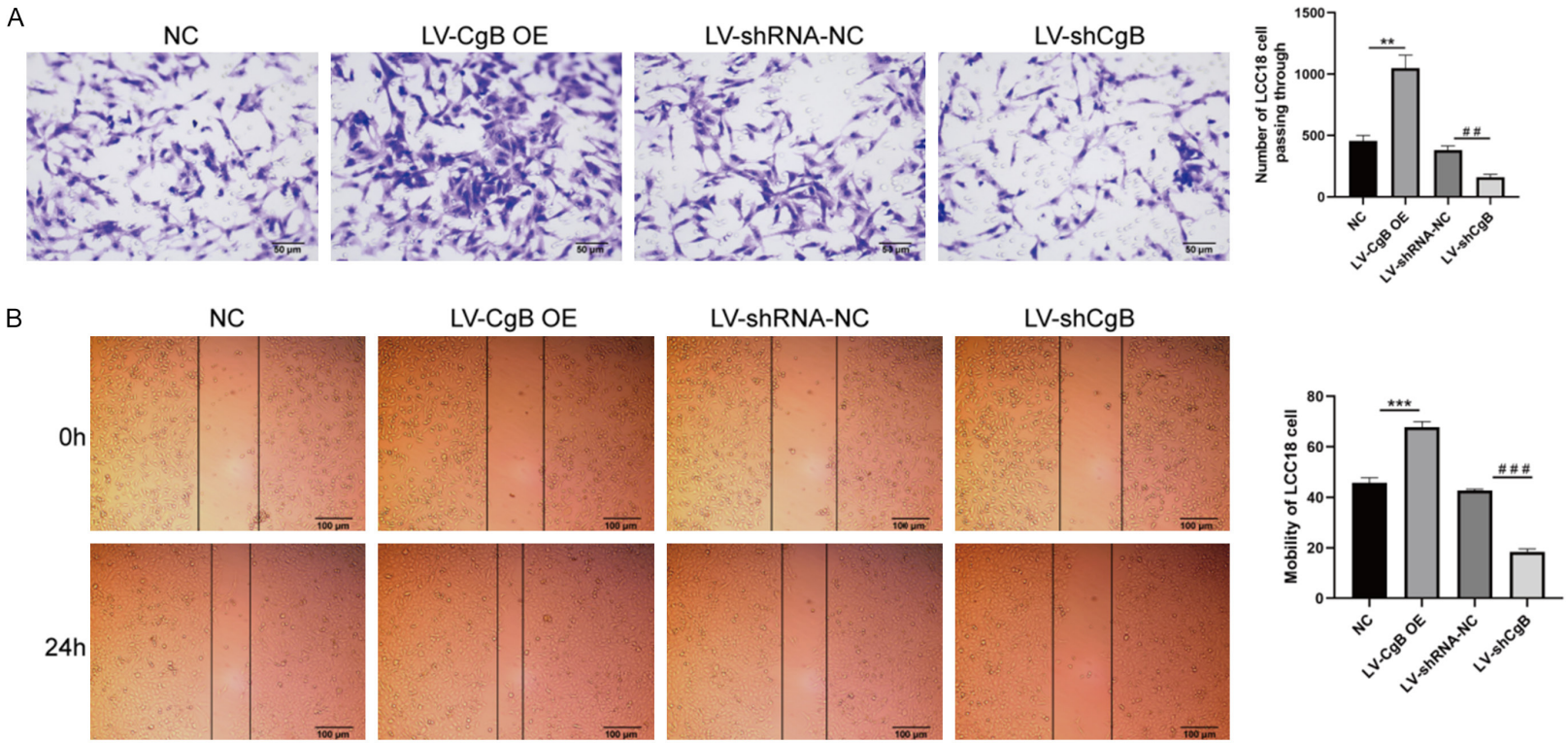

Figure 3. The effect of CgB on the invasion and migration of LCC-18 cells. A. CgB overexpression promoted, while CgB silencing decreased, LCC-18 cell invasion, as determined by Transwell assay (left panel). The bar graph showed the statistically significant difference (right panel). B. Wound healing assay showed the similar effect of CgB on LCC-18 cell migration (left panel). The bar graph of the statistical analysis (right panel). **: P<0.001; ##: P<0.01; ###: P<0.001.

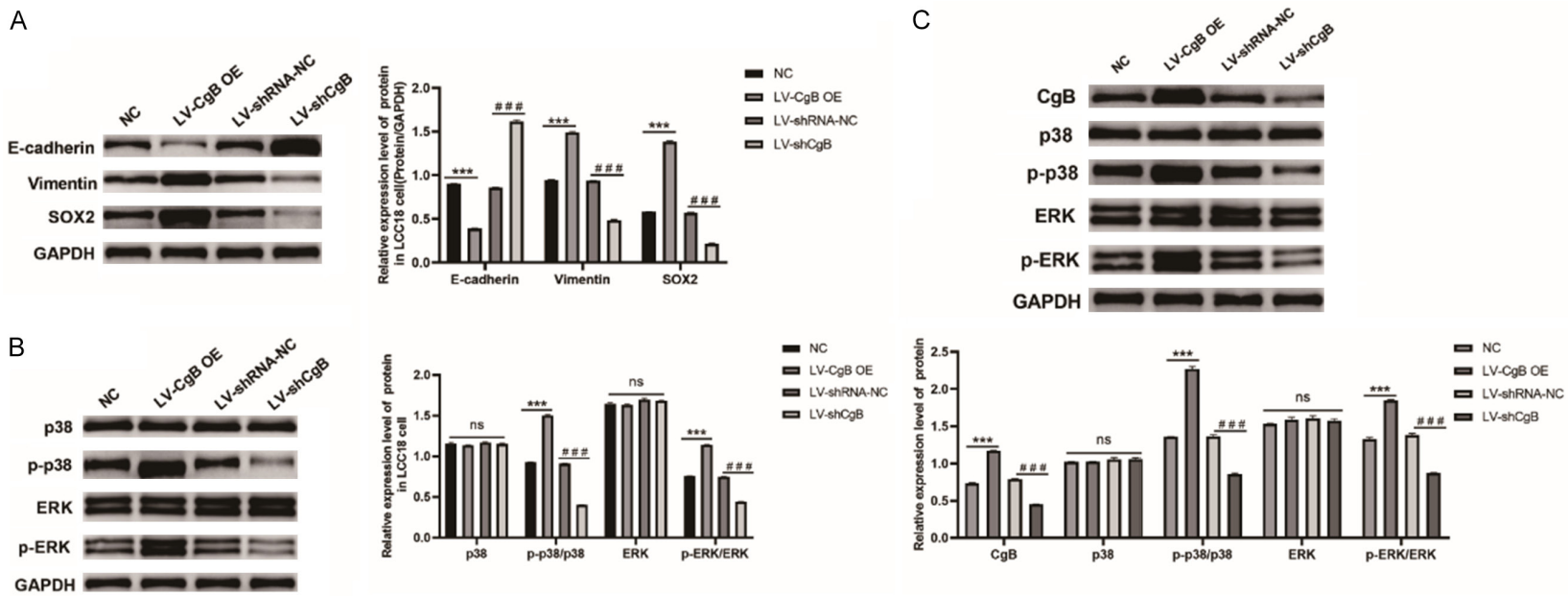

Figure 4. CgB promoted EMT and stemness through the activation of p38 MAPK and ERK pathways. A. Overexpression of CgB significantly suppressed the expression of E-cadherin, while enhanced the expression of Vimentin and SOX2. CgB silencing showed the opposite effect (left panel). The bar graph of the statistical analysis (right panel). B. Upregulation of p-p38 and p-ERK levels by CgB overexpression, while the total protein levels of p38 and ERK were not affected. The protein levels of p-p38 and p-ERK were decreased significantly by CgB silencing (left). The bar chart shows the comparison of relative protein quantity (right), and the difference is statistically significant. C. Western blot analysis of xenograft tumors revealed that the expression of CgB, p-p38, and p-ERK was significantly increased by of CgB overexpression but was decreased by CgB silencing. ***: P<0.001; ###: P<0.001.

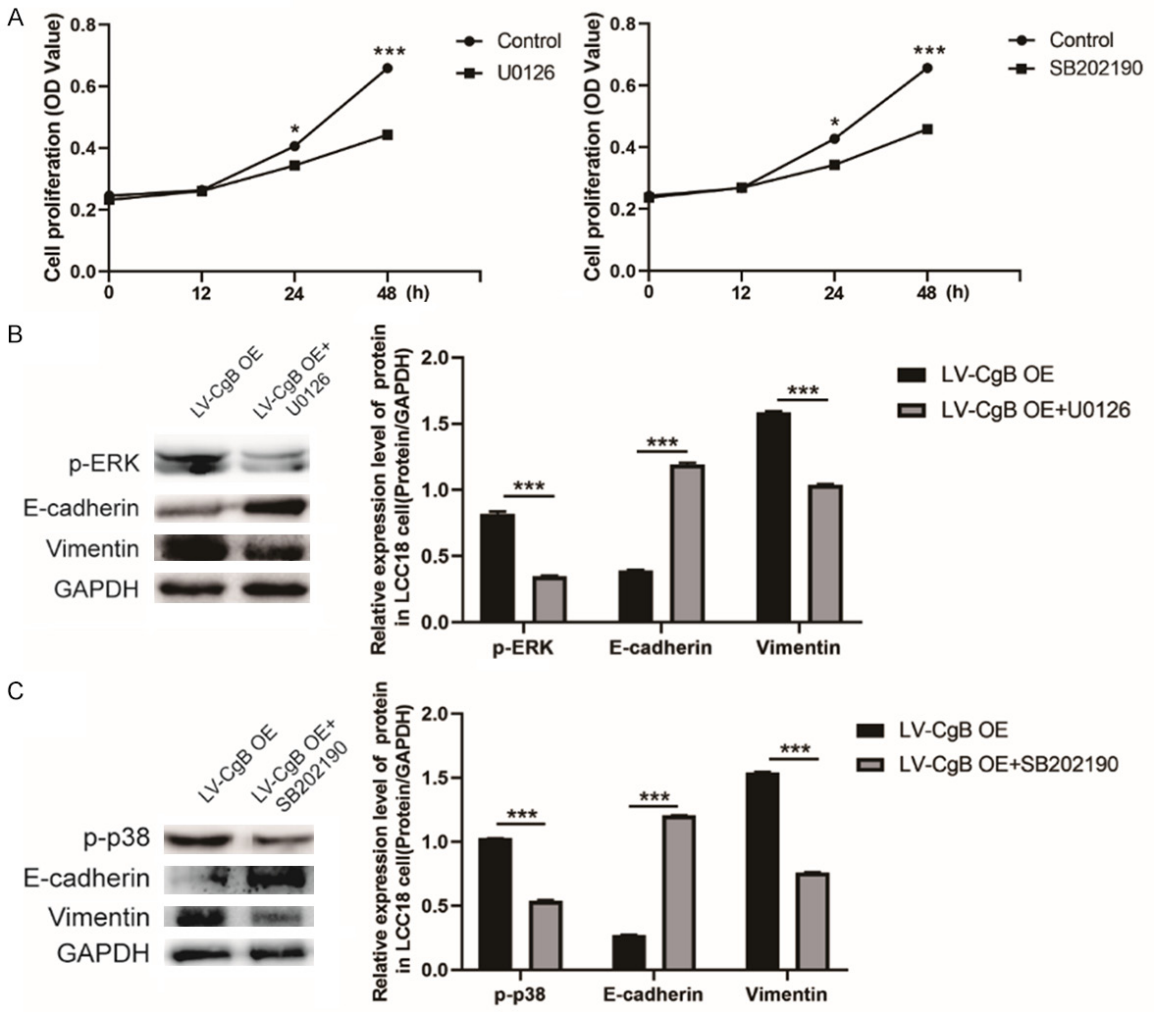

Figure 5. The effects of U0126 and SB202190 on LCC-18 cells. A. LV-CgB OE LCC-18 cells were treated with ERK inhibitor U0126 or p38 inhibitor SB202190 for 6 h, 12 h, 24 h and 48 h, and then cell proliferation was determined by CCK-8 assay. B. LV-CgB OE LCC-18 cells were treated with U0126 (10 μM) for 12 h (U0126 treatment group) or without treatment (control group), and the indicated protein level was detected by Western blot (left panel). Statistical analysis showed the significant difference (right). C. LV-CgB OE LCC-18 cells were treated with SB202190 (20 μM) for 12 h (SB202190 treatment group) or without treatment (control group), and the indicated protein level was detected by Western blot (left panel). Statistical analysis showed the significant difference (right panel). *: P<0.05; ***: P<0.001.

ability of multi-differentiation, which play an important role in promoting tumor metastasis. Studies have confirmed that after normal colonic epithelial cells express mesenchymal characteristics, and the expression of stemness markers are also increased [16]. In addition, it has been reported that injecting prostate cancer tumor cells with stemness characteristics into nude mice will produce highly vascularized neuroendocrine cells and express low levels of E-cadherin, which confirms the relationship among stemness, EMT and neuroendocrinization. Other studies have shown that the over-expression of Snail in prostate cancer cells can lead to EMT and induce neuroendocrine-like morphology, indicated by the increased expression of NSE and CgA increases [17-19]. In line with these findings, our data also demonstrated that overexpression of CgB promoted EMT and stemness.

MAPK/ERK signaling pathways consist of a series of cytoplasmic proteins, including Ras, MAPK kinase-kinase (A-Raf, B-Raf and Raf-1), MAPK kinase (MEK1, MEK2), which transduce signals to ERK1 and ERK2 [20]. MAPK/ERK sig-

nal pathways play an important role in cell proliferation [21]. In addition, MAPK/ERK signaling pathways participate in metastasis process [22, 23]. p38 MAPKs are a family of "stress-activated" serine/threonine kinase. Their activation enables cells to respond to external signals and exert a large number of different biological effects in a tissue-specific and signal-dependent manners, such as inflammation, differentiation, cell proliferation and survival. Notably, p38 MAPKs play a dual role in tumor development as they can mediate cell survival or promote cell death by different mechanisms. A study has shown that p38 MAPKs participate in maintaining the survival and proliferation of colorectal cancer cells [24]. The migration and invasion of cancer cells are also affected by p38 MAPKs [25]. Similarly, MAPK signaling pathway is also involved in colorectal NEN. Studies have shown that ERK1/2 is activated in gastrointestinal NEN [26, 27], which is consistent with our data that CgB regulated the progression of colonic NEC by promoting the activation of p38 MAPK and ERK pathways.

Nevertheless, our study had several limitations. First, this study was a retrospective study with small sample size. In addition, the detailed mechanisms by which CgB regulates the pathogenesis of colonic NEC needs further experimental confirmation.

In conclusion, our study revealed the relationship between CgB expression and the progression of colonic NEC. Our data indicated that CgB might function as an oncogene and serve as a biomarker of colonic NEC. More validation cohorts and further elucidation are needed in to establish the critical role of CgB in cancer development as well as its clinical application in colonic NEC.

Disclosure of conflict of interest

None.

Address correspondence to: Chaoliu Dai, Department of Fifth General Surgery, Shengjing Hospital Affiliated to China Medical University, Shenyang 110004, Liaoning, China. E-mail: 18941651469@163.com; Baolin Liu, Department of Sixth General Surgery, Shengjing Hospital Affiliated to China Medical University, Shenyang 110004, Liaoning, China. E-mail: liubl@sj-hospital.org

References

[1] Volante M, Grillo F, Massa F, Maletta F, Mastracci L, Campora M, Ferro J, Vanoli A and Papotti M. Neuroendocrine neoplasms of the appendix, colon and rectum. Pathologica 2021; 113: 19-27.

[2] Pavel M, Baudin E, Couvelard A, Krenning E, Oberg K, Steinmuller T, Anlauf M, Wiedenmann B and Salazar R; Barcelona Consensus Conference participants. ENETS consensus guidelines for the management of patients with liver and other distant metastases from neuroendocrine neoplasms of foregut, midgut, hindgut, and unknown primary. Neuroendocrinology 2012; 95: 157-176.

[3] Shinji S, Naito Z, Ishiwata T, Tanaka N, Furukawa K, Suzuki H, Seya T, Kan H, Tsuruta H, Matsumoto S, Matsuda A, Teranishi N, Ohaki Y and Tajiri T. Neuroendocrine cell differentiation of poorly differentiated colorectal adenocarcinoma correlates with liver metastasis. Int J Oncol 2006; 29: 357-364.

[4] Helle KB. The granin family of uniquely acidic proteins of the diffuse neuroendocrine system: comparative and functional aspects. Biol Rev Camb Philos Soc 2004; 79: 769-794.

[5] Benedum UM, Lamouroux A, Konecki DS, Rosa P, Hille A, Baeuerle PA, Frank R, Lottspeich F, Mallet J and Huttner WB. The primary structure of human secretogranin I (chromogranin B): comparison with chromogranin A reveals homologous terminal domains and a large intervening variable region. EMBO J 1987; 6: 1203-1211.

[6] Montero-Hadjadje M, Vaingankar S, Elias S, Tostivint H, Mahata SK and Anouar Y. Chromogranins A and B and secretogranin II: evolutionary and functional aspects. Acta Physiol (Oxf) 2008; 192: 309-324.

[7] Bartolomucci A, Possenti R, Mahata SK, Fischer-Colbrie R, Loh YP and Salton SR. The extended granin family: structure, function, and biomedical implications. Endocr Rev 2011; 32: 755-797.

[8] Laguerre F, Anouar Y and Montero-Hadjadje M. Chromogranin A in the early steps of the neurosecretory pathway. IUBMB Life 2020; 72: 524-532.

[9] Borges R, Diaz-Vera J, Dominguez N, Arnau MR and Machado JD. Chromogranins as regulators of exocytosis. J Neurochem 2010; 114: 335-343.

[10] Uhlen M, Fagerberg L, Hallstrom BM, Lindskog C, Oksvold P, Mardinoglu A, Sivertsson A, Kampf C, Sjostedt E, Asplund A, Olsson I, Edlund K, Lundberg E, Navani S, Szigyarto CA, Odeberg J, Djureinovic D, Takanen JO, Hober S, Alm T, Edqvist PH, Berling H, Tegel H, Mulder J,

Rockberg J, Nilsson P, Schwenk JM, Hamsten M, von Feilitzen K, Forsberg M, Persson L, Johansson F, Zwahlen M, von Heijne G, Nielsen J and Ponten F. Proteomics. Tissue-based map of the human proteome. Science 2015; 347: 1260419.

[11] Miki M, Ito T, Hijioka M, Lee L, Yasunaga K, Ueda K, Fujiyama T, Tachibana Y, Kawabe K, Jensen RT and Ogawa Y. Utility of chromogranin B compared with chromogranin A as a biomarker in Japanese patients with pancreatic neuroendocrine tumors. Jpn J Clin Oncol 2017; 47: 520-528.

[12] Sekiya K, Ghatei MA, Salahuddin MJ, Bishop AE, Hamid QA, Ibayashi H, Polak JM and Bloom SR. Production of GAWK (chromogranin-B 420-493)-like immunoreactivity by endocrine tumors and its possible diagnostic value. J Clin Invest 1989; 83: 1834-1842.

[13] Stridsberg M, Eriksson B, Fellstrom B, Kristiansson G and Tiensuu Janson E. Measurements of chromogranin B can serve as a complement to chromogranin A. Regul Pept 2007; 139: 80-83.

[14] Li YL, Wang X, Wang P, Han D, Li XK, Jiao PP, Qi ZR, Wang C, Shi YF and Tan HY. The role of chromogranin B in advanced neuroendocrine tumors. Chinese Journal of the Frontiers of Medical Science (Electronic Version) 2021; 13: 40-44.

[15] Nieto MA. The ins and outs of the epithelial to mesenchymal transition in health and disease. Annu Rev Cell Dev Biol 2011; 27: 347-376.

[16] Findlay VJ, Wang C, Watson DK and Camp ER. Epithelial-to-mesenchymal transition and the cancer stem cell phenotype: insights from cancer biology with therapeutic implications for colorectal cancer. Cancer Gene Ther 2014; 21: 181-187.

[17] McKeithen D, Graham T, Chung LW and Odero-Marah V. Snail transcription factor regulates neuroendocrine differentiation in LNCaP prostate cancer cells. Prostate 2010; 70: 982-992.

[18] Conteduca V, Aieta M, Amadori D and De Giorgi U. Neuroendocrine differentiation in prostate cancer: current and emerging therapy strategies. Crit Rev Oncol Hematol 2014; 92: 11-24.

[19] Salvatori L, Caporuscio F, Verdina A, Starace G, Crispi S, Nicotra MR, Russo A, Calogero RA, Morgante E, Natali PG, Russo MA and Petrangeli E. Cell-to-cell signaling influences the fate of prostate cancer stem cells and their potential to generate more aggressive tumors. PLoS One 2012; 7: e31467.

[20] De Luca A, Maiello MR, D'Alessio A, Pergameno M and Normanno N. The RAS/RAF/MEK/ERK and the PI3K/AKT signalling pathways: role in cancer pathogenesis and implications for therapeutic approaches. Expert Opin Ther Targets 2012; 16 Suppl 2: S17-27.

[21] Dong C, Davis RJ and Flavell RA. MAP kinases in the immune response. Annu Rev Immunol 2002; 20: 55-72.

[22] Yang W, Redpath RE, Zhang C and Ning N. Long non-coding RNA H19 promotes the migration and invasion of colon cancer cells via MAPK signaling pathway. Oncol Lett 2018; 16: 3365-3372.

[23] Xiang T, Fei R, Wang Z, Shen Z, Qian J and Chen W. Nicotine enhances invasion and metastasis of human colorectal cancer cells through the nicotinic acetylcholine receptor downstream p38 MAPK signaling pathway. Oncol Rep 2016; 35: 205-210.

[24] Chiacchiera F and Simone C. Inhibition of p38alpha unveils an AMPK-FoxO3A axis linking autophagy to cancer-specific metabolism. Autophagy 2009; 5: 1030-1033.

[25] Chiacchiera F, Grossi V, Cappellari M, Peserico A, Simonatto M, Germani A, Russo S, Moyer MP, Resta N, Murzilli S and Simone C. Blocking p38/ERK crosstalk affects colorectal cancer growth by inducing apoptosis in vitro and in preclinical mouse models. Cancer Lett 2012; 324: 98-108.

[26] Karhoff D, Sauer S, Schrader J, Arnold R, Fendrich V, Bartsch DK and Horsch D. Rap1/B-Raf signaling is activated in neuroendocrine tumors of the digestive tract and Raf kinase inhibition constitutes a putative therapeutic target. Neuroendocrinology 2007; 85: 45-53.

[27] Briest F and Grabowski P. PI3K-AKT-mTOR-signaling and beyond: the complex network in gastroenteropancreatic neuroendocrine neoplasms. Theranostics 2014; 4: 336-365.

Supplementary Table 1. Information of the RT-PCR primer sequences

	Forward (5' to 3')	Reverse (5' to 3')
β-actin	CACTGTGCCCATCTACGAGG	TAATGTCACGCACGATTTCC
CgB	CTGGCTGTGGAGAAGGAGG	AGCGCACATCGCGGTAG